

Breaking the sound barrier in recombination fronts

R.J.R. Williams & J.E. Dyson

Department of Physics and Astronomy, University of Manchester, Oxford Road, Manchester M13 9PL

Received ****INSERT****; in original form ****INSERT****

ABSTRACT

We exploit a generic instability in the integration of steady, sonic, near-isothermal flows to find the complete transition diagram for recombination fronts (for a model system of equations). The instability requires the integration of the flow equations for speeds between the isothermal and adiabatic sound speeds to be performed with particular care. As a result of this, the previous work of Newman & Axford on the structure of recombination fronts neglected an important class of solution, that of transonic fronts; our method is readily extensible to a more complete treatment of the ionization structure. Future papers will apply these results in models of the structure of ultracompact H II regions.

Key words: hydrodynamics – stars: mass-loss – ISM: structure – H II regions

1 INTRODUCTION

The hydrodynamics of gas photoionized by a central star has been widely studied (e.g. Kahn 1954; Axford 1961; Goldsworthy 1961). The gas is almost completely ionized close to the central source. The incident radiation field decreases with radius as a result of geometrical divergence and because atomic recombination always results in a small population of neutral atoms, which have finite opacity to the ionizing radiation. At some radius the gas becomes optically thick to the ionizing radiation, and beyond this radius it is predominantly neutral.

The transition between ionized and neutral gas can be treated as a quasi-steady, plane-parallel front when it takes place over a small distance, compared with the radius of the region, and can be included in models of the global flow as a discontinuity (e.g. Osterbrock 1989). This is, in general, the appropriate case for ionization fronts (IF), since the opacity of the gas to ionizing radiation increases rapidly as a function of decreasing ionization. In this paper, we will distinguish recombination fronts (RF) from IF as the case when the net flow of gas is from high ionization towards low ionization. RF can be broadened significantly by the advection of ionized gas, whereas IF are generally only as thick as the (small) photon mean free path in neutral gas.

Newman & Axford (1968 – henceforth NA) studied the possible RF transitions in the context of stellar winds. They found that thin fronts were unlikely to occur in the winds of solar-type stars but might be important in the ejecta of planetary nebulae. In recent studies of ultracompact H II regions (Dyson 1994; Williams & Dyson 1994; Dyson, Williams & Redman 1995), we have discussed the likely importance of (thin) RF in the flow structures. In particular, the likely coincidence of RF and sonic transitions raised some questions

with regard to the work of NA, which we address in this paper.

The significance of the small class of steady solutions which pass through sonic transitions at the RF is perhaps not immediately apparent when only conditions close to the front are considered. However, such solutions become important when the front is included in the global solution of an initially subsonic divergent flow. Here, the ballistic character of the supersonic solutions allows such ‘winds’ to satisfy a wide range of external pressure boundary conditions, by the inclusion of a shock at some radius, for external pressures far lower than required if the solutions are subsonic at all radii (Parker 1958).

As part of this study, we also address the apparent paradox that for conditions arbitrarily close to isothermal, the flow equations are singular at the *adiabatic* sound speed, whereas in the isothermal limit they are singular at the *isothermal* sound speed.

In the following sections, we give simple model equations for steady ionized gas flow, and derive a second order system which describes the structure of plane IF and RF. A reorganisation of these equations suggests that for a narrow range of flow speeds in the region where the flow is nearly isothermal, a formal instability will prevent direct integration of the Mach number equation in the downstream direction; this is illustrated by a yet simpler model system. With this in mind, we return to RF, and find a range of transonic solutions which were inadvertently missed by NA. In conclusion, we briefly discuss the relevance of these results to models of ultra compact H II regions, and note possible implications of our study for the details of the evolution of conventional IF in H II regions at the time of shock generation.

2 BASIC EQUATIONS

Differential equations for the structure of ionization and recombination fronts are given by NA (cf. also Frank, Noriega-Crespo & Balick 1992). Terms which account for photoionization and recombination, the radiative transfer of ionizing radiation and the heating and cooling of the gas are added to the basic equations of hydrodynamics. The processes included are ionization of atomic hydrogen, proton and electron recombination in the on-the-spot approximation, and an approximation to forbidden line cooling (L_{ei}). Mason (1977) gives far more detailed models of the internal structure of several types of IF, showing, for example, the ionization structure of O, N and Ne. For the present paper, however, the approximations of NA will suffice.

The following equations give a reasonable approximation to the structure of RF, in the frame in which the front is steady, (cf. Axford 1961; NA):

$$\nabla \cdot (\rho \mathbf{v}) = 0 \quad (1a)$$

$$\nabla \cdot ([\rho \mathbf{v}] \mathbf{v}) = -\nabla p \quad (1b)$$

$$\nabla \cdot \left(\left[w + \frac{1}{2} \rho v^2 \right] \mathbf{v} \right) = \rho Q \quad (1c)$$

$$\nabla \cdot ([\rho x] \mathbf{v}) = \rho [(\alpha J)(1-x) - \beta n x^2] \quad (1d)$$

$$\nabla \cdot \mathbf{J} = -n(\alpha J)(1-x), \quad (1e)$$

where ρ is the mass-density in the gas, \mathbf{v} is the velocity, p is the pressure and x is the fractional ionization. The equation of state,

$$p = (1+x)n k T, \quad (2)$$

relates these quantities to $n = \rho/m_H$, the nucleon number density, and the gas temperature T . The photoionization cross-section of hydrogen at the Lyman limit is taken to be $\alpha = 6.3 \times 10^{-18} \text{ cm}^2$ per atom, and β , the case B recombination coefficient, is $\beta_0 T^{-3/4}$, where we use the value $\beta_0 = 3 \times 10^{-10} \text{ cm}^3 \text{ s}^{-1} \text{ K}^{3/4}$ from NA.

The internal energy per unit volume is $\epsilon = p/(\gamma - 1)$; the enthalpy per unit volume is $w = \epsilon + p$. $\mathbf{J} \equiv J \hat{\mathbf{r}}$ is the outward flux of ionizing photons.

Q is an effective heating rate, given by

$$\rho Q = k T_* n (\alpha J)(1-x) - \frac{1}{\gamma-1} \beta k T n^2 x^2 - n^2 x^2 L_{ei}, \quad (3)$$

where T_* is the effective stellar temperature (which we take to be 40 000 K). The final term in equation (3) is a fit to forbidden line cooling (Goldsworthy 1961), where

$$L_{ei} = \begin{cases} L_{ei0}(T - 4000 \text{ K})^2 & \text{for } T > 4000 \text{ K} \\ 0 & \text{otherwise} \end{cases} \quad (4)$$

and $L_{ei0} = 9.7 \times 10^{-32} \text{ erg cm}^3 \text{ s}^{-1} \text{ K}^{-2}$. This fit is poor for gas temperatures above 10^5 K , but since temperatures as high as this are not found in the fronts that we are studying, and since we wish to compare our results to those of NA, we defer a more accurate treatment of forbidden line cooling to the future.

Boundary conditions (at small r) are of high ionization ($x \rightarrow 1$), high ionizing flux ($J \rightarrow \infty$), equilibrium temperature ($Q \rightarrow 0$) and an arbitrary initial velocity ($v > 0$). These are, however, not sufficient to fully determine the flow in all cases, as will be described below.

3 STEADY STATE SOLUTIONS

For a thin front, the mass flux and momentum equations (1a, 1b) can be integrated immediately. The remaining ordinary differential equations which describe the front are

$$\frac{dm}{dr} = \frac{1 + \gamma m^2}{1 - m^2} \left(\frac{(\gamma - 1)Q}{2c^3} \right) \quad (5a)$$

$$\frac{dx}{dr} = n \left(\alpha j(1-x) - \frac{\beta x^2}{v} \right) \quad (5b)$$

$$\frac{dj}{dr} = -n \alpha j(1-x), \quad (5c)$$

where c is the adiabatic sound speed, $c^2 = \gamma p/\rho$, m is the *adiabatic* Mach number, and $j \equiv J/nv$ is the dimensionless ionizing flux. The integrals of the mass and momentum flux equations, Φ and Π respectively, are

$$\Phi = \rho v; \quad \Pi = \left[\frac{1}{\gamma} + m^2 \right] \rho c^2. \quad (6)$$

Hence $\Pi/\Phi = (1 + \gamma m^2)c/\gamma m$. In this system of equations, the radial distance scales simply with density, and so we can study two coupled ODEs for dm/dj and dx/dj which are equivalent to the equations studied by NA.

3.1 A numerical instability of near-isothermal sonic flows

Using equations (6) to relate m to c , we can rearrange equation (5a) into the suggestive form:

$$v \frac{d \ln(c^2)}{dr} = \frac{1 - \gamma m^2}{1 - m^2} (\gamma - 1) Q / c^2, \quad (7)$$

(cf. also equation (15) of Williams, Hartquist & Dyson, 1995). If the level of ionization is weakly varying, then $c^2 \propto T$. For substantially subsonic flows ($m \ll 1$) and for supersonic flows ($m > 1$) the solution will tend to relax to a stable equilibrium as we integrate in the downstream direction. For our system of equations, the flow reaches equilibrium at a temperature $T \simeq 7800 \text{ K}$ (cf. NA).

However, when the flow velocity is in the range between the isothermal sound speed (i.e. $m = 1/\sqrt{\gamma}$) and the adiabatic sound speed ($m = 1$), the first factor on the r.h.s. of equation (7) is negative: thermally stable equilibria appear to become unstable (when the flow is integrated downstream) and vice versa (so long as the dynamical time, $(dv/dr)^{-1}$, is much longer than the thermal timescale, $\sim c^2/Q$).

This behaviour is readily understood in terms of the formation of weak ‘isothermal shocks’ in the flow. If the flow were *strictly* isothermal, discontinuous shocks could form with upstream Mach numbers in the unstable range (cf. Figure 4). For finite cooling, discontinuous solutions no longer exist. The instability of the equilibrium solution nevertheless allows the flow to decrease its Mach number through a *resolved* transition at any point, and since the flow properties upstream and downstream of this transition satisfy the isothermal Rankine-Hugoniot relations, we refer to these transitions as resolved isothermal shocks.

We illustrate this in Figure 1 for the simpler case of a steady plane flow with no ionization, using a simple heating function $Q \propto (T_e - T)$ in equation (5a), where T_e is the

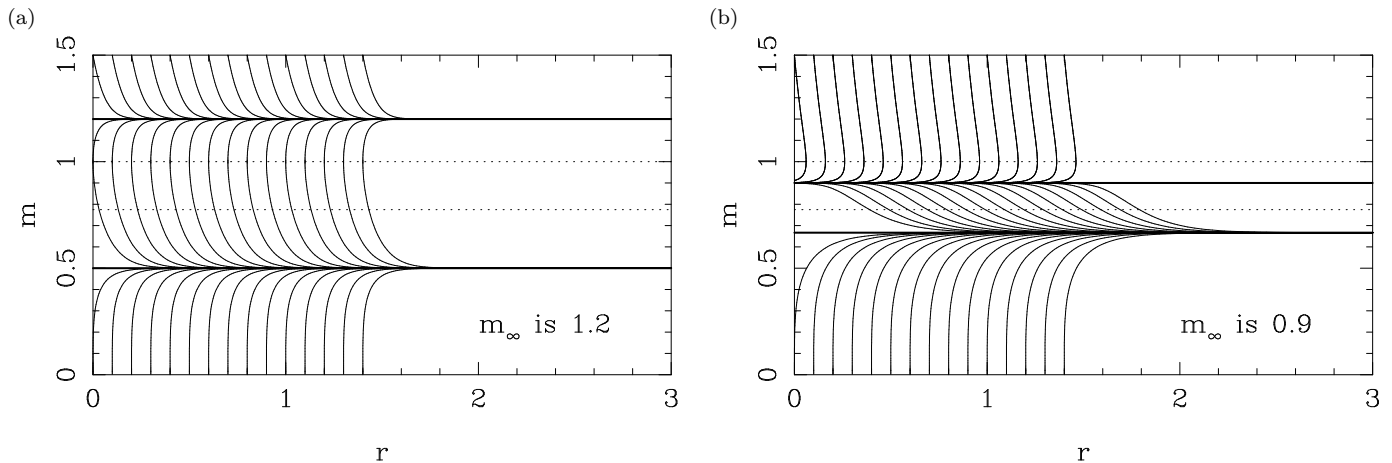


Figure 1. Steady solutions of flows with heating $Q \propto T_e - T$ for (a) $m_\infty = 1.2$ and (b) $m_\infty = 0.9$. The flow direction is towards increasing r . The bold, horizontal lines are the equilibrium solutions. Dotted lines mark the isothermal and adiabatic sound speeds.

equilibrium temperature. The plot shows rest frame solutions, with the integration performed downstream, towards increasing r . The solutions are independent of r , but a range of solutions are shown arbitrarily offset in this direction to indicate the morphology of solutions expected in more complicated situations.

Note that in this model, Q is independent of ρ . This cooling law is stable to equilibrium perturbations, and also marginally stable to the instabilities of algebraic power within cooling zones (Field 1965; Fall & Rees 1985). Since the peak temperatures found within the isothermal shocks are less than 3 per cent above the equilibrium temperature, we can safely ignore this marginal instability; in any case, the results are similar for $Q \propto (T_e^n - T^n)$ with $n > 1$.

We first show a case for which both the sub- and the supersonic solutions to the flow equations integrate stably, with $m_\infty = 1.2$ (or, equivalently, $m_\infty = 0.5$). In Figure 1a, the bold, horizontal lines are the equilibrium solutions; thinner solid lines show solutions integrated downstream (to the right) from an initial non-equilibrium state. The isothermal and adiabatic sound speeds are shown as dotted lines. As we integrate downstream, sub- (super-) sonic initial conditions relax to the sub- (super-) sonic equilibrium solution.

Figure 1b is for $m_\infty = 0.9$ (or, equivalently, $m_\infty \simeq 0.67$). Here, we see that the equilibrium solution $m = 0.9$ is apparently unstable as we integrate downstream (left to right), with solutions diverging to large m and towards the $m \simeq 0.67$ equilibrium. These latter solutions are, in effect, weak shocks. If we consider a Galilean transformation of the system, it is apparent that the instability found is entirely a result of the steady-state assumption: $m = 0.9$ is a perfectly reasonable equilibrium solution, as is confirmed by time-dependent simulations of such flows. For some downstream conditions, however, it will be necessary for a weak shock to form in the flow at some (in the present case, arbitrary) position. The instability demonstrated here allows this to occur in continuous solutions, just as discontinuous adiabatic Rankine-Hugoniot shocks can form at arbitrary positions in flows initially above the adiabatic sound speed.

Since downstream integration of these ODEs for initial conditions perturbed from equilibrium confirms the ex-

istence of rapidly divergent solutions for flows between the isothermal and adiabatic sound speeds, we conclude that the solutions found by Newman & Axford (NA) in this range of upstream Mach numbers inadvertently included these weak isothermal shocks. In the next section, we present the additional transonic solutions this led them to disregard.

3.2 Structure of recombination fronts

The presence of the instability discussed in the previous section in the downstream integration of near isothermal flows implies that, when the upstream flow is between the isothermal and adiabatic sound speeds, the initial conditions $m \rightarrow m_\infty$, $x \rightarrow 1$ at $j \rightarrow \infty$ used by Newman & Axford *do not fully specify* the flow solutions. In this section, we use this freedom to find an important class of RF overlooked by NA – transonic fronts. In what follows, we return to the full model equations (5a-c) for the structure of RF.

In looking for transonic solutions, where $Q = 0$ and $v(dQ/dr) < 0$ at $m = 1$ (so the flow can pass smoothly through the adiabatic sound speed), we have formulated a two-point boundary problem (with conditions applied both far upstream in the H II flow and at the sonic point). We have indicated that for initial conditions $1/\sqrt{\gamma} < m < 1$, the Mach equation is unstable when integrated downstream. However, the ionization equation is highly unstable when integrated in the opposite, upstream direction.

The vigorousness of these instabilities precludes the use of shooting methods. We therefore employed an iterative procedure to find the flow solution between $j \rightarrow \infty$ and the adiabatic sonic point (outside this region, downstream integration proceeds smoothly). An approximation to the ionization structure was determined by downstream integration. Using this approximation to the ionization structure, the equation for the Mach number was integrated upstream. This gave an updated model for the velocity and sound speed distributions, which were then used to derive an updated ionization structure: this procedure was iterated to convergence.

The integrations were performed with a stiff ODE integration package (Cohen & Hindmarsh 1994), using cubic

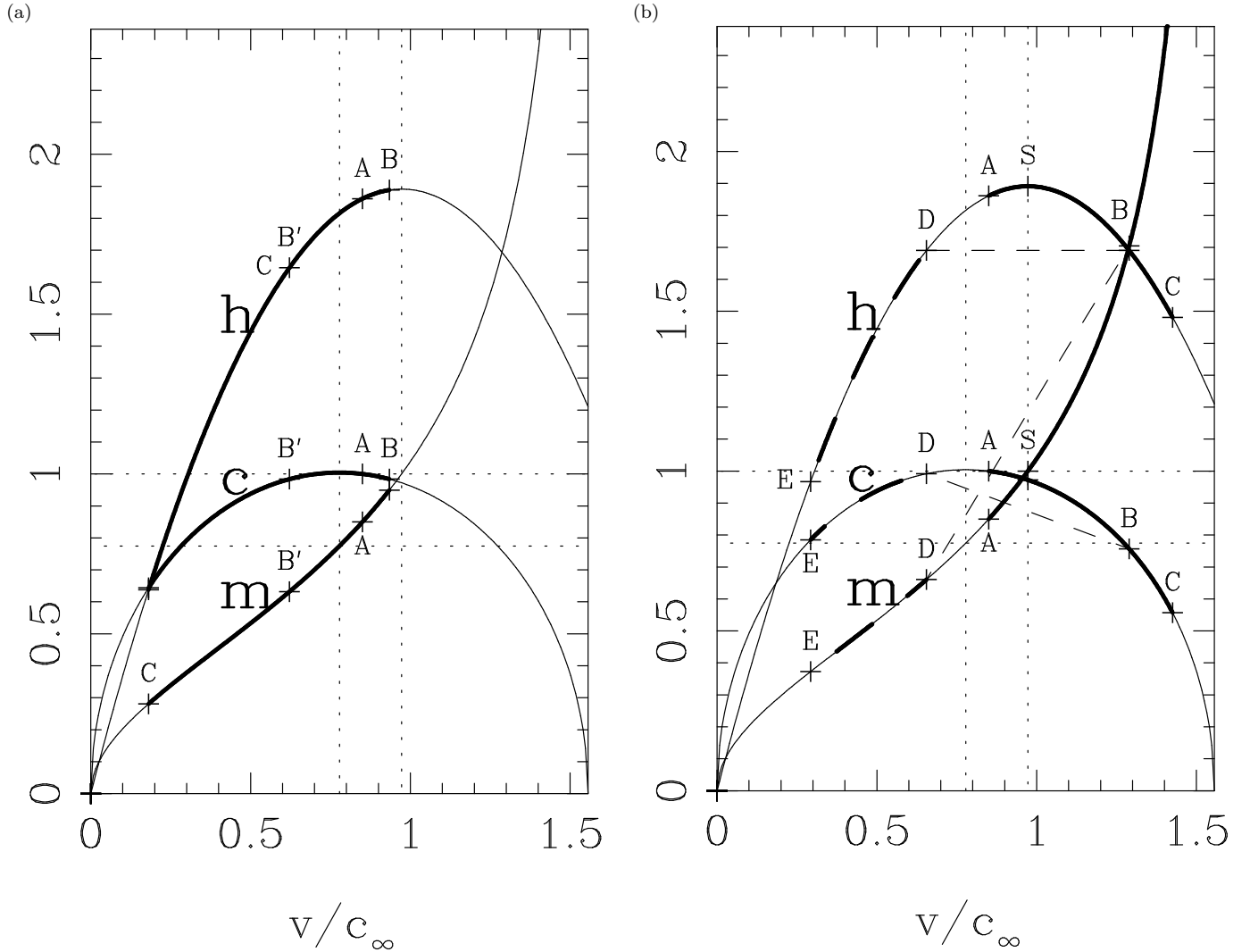


Figure 3. Example solutions for $m_\infty = 0.85$. The enthalpy (h , in units of c_∞^2), sound speed (c in units of c_∞) and adiabatic Mach number (m) are plotted against the flow velocity (u in units of c_∞). Vertical dotted lines mark the maximum of c , where the flow is at the isothermal sound speed, and the maximum of h , where the flow is at the adiabatic sound speed; horizontal dotted lines mark the values of m at these speeds. In case (a) an ‘isothermal shock’ is formed ahead of the sonic point (the flow travels $A \rightarrow B$ then passes through the isothermal shock $B \rightarrow A \rightarrow B'$ and then recombines and cools to reach C in the end). Case (b) includes a sonic point (S) – the solution with no shock is $A \rightarrow S \rightarrow B \rightarrow C$, but there are also solutions such as $A \rightarrow S \rightarrow B \rightarrow D \rightarrow E$ which include an adiabatic shock ($B \rightarrow D$, shown dashed).

spline interpolation of the results. The singular equations for dm/dj and dx/dj were split into non-singular equations in a dummy independent variable s (i.e. for dm/ds , dx/ds and dj/ds).

In Figure 2 we show one such transonic solution, for upstream Mach number $m_\infty = 0.85$. The solid bold curve is the Mach number of the transonic solution, plotted as a function of the ionization fraction, x . Also shown in this figure are the distributions of dimensionless ionizing flux j , sound speed c , temperature T , velocity v and stagnation enthalpy, $h = c^2/(\gamma - 1) + v^2/2$, through the front. Note that all these curves are smooth, and that h has a maximum value when $m = 1$, as expect (cf. Figure 3).

In Figure 3, we show the various classes of solution perturbed from the transonic case. The three curves on the plots show the adiabatic Mach number, m , sound speed, c , and

enthalpy h as a function of flow velocity, v . In Figure 3a, a solution with a weak isothermal shock is shown. From the initial point A , the flow cools and accelerates. However, an isothermal shock is triggered at point B , and the flow then heats again and slows. As the shock is resolved, the solution remains on the integral curves at all times – the part of the curve between points B and B' might, however, be considered to represent the isothermal shock. Beyond the shock, in the region $B' \rightarrow C$, the flow decelerates and cools further as the gas recombines.

Figure 3b illustrates a transonic solution, $A \rightarrow S \rightarrow B \rightarrow C$. Here, the flow has been chosen to accelerate smoothly through sonic point S , at the maximum of the enthalpy h . Beyond the sonic point, the flow accelerates, cools and recombines to reach point C when it has become fully neutral. Also illustrated is the solution which results when

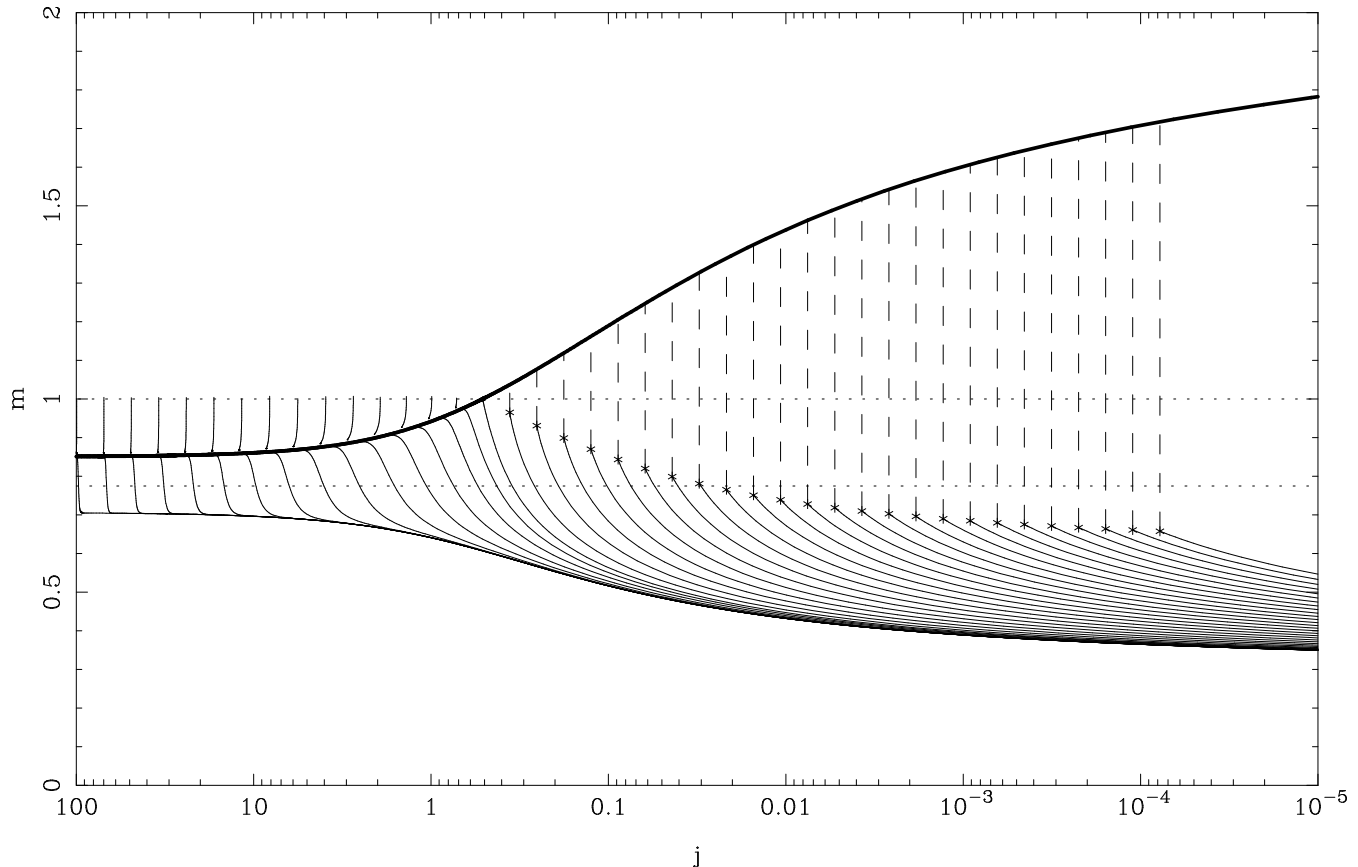


Figure 4. Steady solutions for an RF with Mach number $m_\infty = 0.85$ far upstream (at high ionizing flux, to the left of this plot) in the ionized gas. The bold curve is the transonic solution. A sample of the solutions divergent from the transonic case are shown for initial points upstream of the sonic point. Downstream of the sonic point, solutions are shown, perturbed by an initial steady adiabatic shock (shown dashed). Horizontal dotted lines mark the isothermal and adiabatic sound speeds. For the subsonic downstream solutions, final temperatures vary between 6500 K (for flows which shock far upstream in the H II region) and 14000 K (where the gas shocks far downstream in the H I region).

an adiabatic shock occurs at point B, taking the flow discontinuously to D. Beyond D, the flow behaves in a similar fashion to that illustrated for the isothermal shock case in Figure 3a, except that it does not reach quite such a low temperature as it approaches infinity.

In Figure 4 we plot the flow Mach number, m , for a wide range of these solutions against the dimensionless ionizing flux, j . Upstream of the sonic point, both the physical solution (which continues subsonically to $j \rightarrow 0$) and the unphysical solution (which tends to $m = 1$ with infinite gradient) are shown. At large j , these solutions diverge very sharply, underlining the difficulty in finding transonic solutions by shooting methods. Beyond the sonic point, solutions are shown for initial conditions found downstream of steady adiabatic shocks (shown dashed) which are now allowed. These shocked solutions form a one-parameter family in combination with the physical solutions which diverge from the transonic solution upstream of the sonic point: as the stepping-off point of these solutions moves progressively downstream, the maximum in Mach number of the divergent solutions becomes a cusp at the sonic point, and then a discontinuity (i.e. shock). A range of final Mach numbers results from this range of solutions.

In Figure 5 we show the transition diagram from Mach number m_2 in the H II flow (at the equilibrium temperature) far upstream to Mach number m_1 in the downstream H I flow. In this diagram, we plot both the results we obtained following Newman & Axford, and the extra solutions found in this work. The short segment of the upper right hand branch of solutions shown bold, between dotted horizontal lines at the isothermal and adiabatic sound speeds, give the transonic solutions. Additional regions of subsonic solutions to the top left result both from shocks downstream of the sonic point in transonic solutions, and from the use of isothermal, rather than adiabatic, shock relations for shocks forming in the H II region.

To interpret this diagram, it is useful to remember that because the upstream flow is assumed to be at the fixed equilibrium temperature, the curves plotted are for a *family* of ODEs, parameterised by Π/Φ . Isothermal shock conditions $m_+m_- = 1/\gamma$ relate the values of m_2 where the ODEs are identical. The sudden appearance of extra solutions with $m_1 > 1$ at $m_2 = 1/\sqrt{\gamma}$ is allowed because this is the singular value where Π/Φ is a minimum.

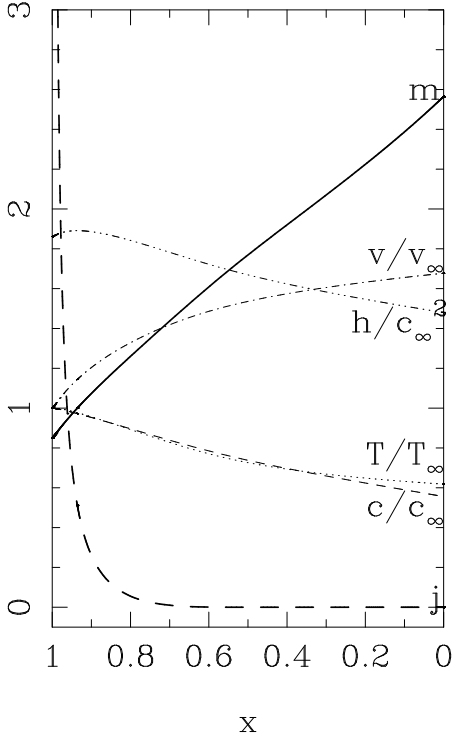


Figure 2. Transonic solution for an RF with Mach number $m_\infty = 0.85$ far upstream in the ionized gas. The Mach number m , dimensionless flux j , sound speed c , temperature T , flow velocity v and specific enthalpy h are plotted against ionization fraction x . This solution here has $j_{\text{son}} = 0.51$ and $x_{\text{son}} = 0.936$, and the Mach number of the H I flow far downstream is $m_1 = 2.56$, corresponding to a temperature there of 4800 K.

4 CONCLUSIONS

In this paper, we have completed the solution space found by Newman & Axford (NA) for recombination front flows. Careful treatment of the numerical integration for flow speeds between the isothermal and adiabatic sound speeds reveals an extra class of transonic solutions overlooked by these authors.

Close to the sonic point, the form of these solutions is similar to those found for any steady transonic flow, for instance a Parker (1958) wind. The steady, transonic solution can in general be found by integrating away from the sonic point. However, inclusion of ionization equilibrium means that we must treat a two-point boundary value problem. The strength of the instability discussed above adds significantly to the usual difficulties integrating the Mach number equation towards a nodal solution, rendering shooting methods impractical and allowing transonic solutions to be easily overlooked. We overcome this difficulty with an iterative scheme, integrating separate equations in the upstream and downstream directions.

The instability in downstream integration adds a free parameter to the solution, resolving the conceptual difficulty of how, as the initial Mach number of our solution increases through isothermal Mach 1, the flow solution changes from an initial-value to a two-point boundary problem. Moreover, these solutions give some insight into the apparent paradox that, for finite cooling, the singularity in steady flow equa-

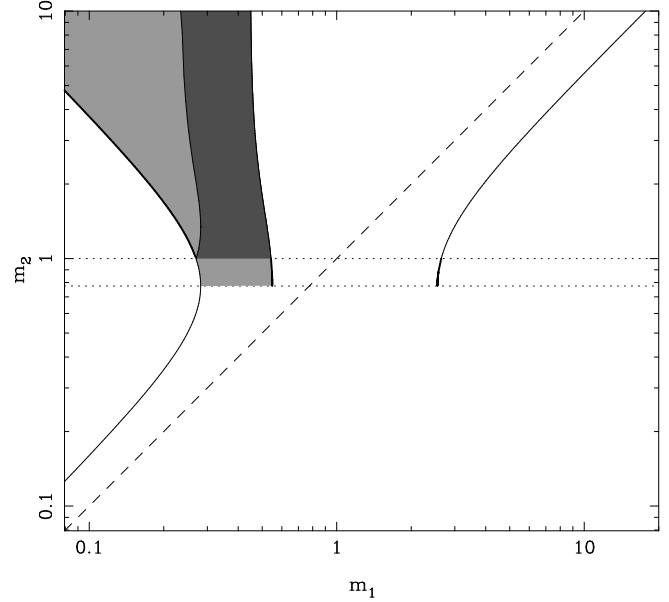


Figure 5. Transition diagram for RF (cf. Figure 5 of NA). Here m_2 is the adiabatic Mach number far upstream in the H II flow, m_1 is the adiabatic Mach number far downstream in the H I flow. The dashed line is $m_1 = m_2$; dotted lines mark where the upstream flow is at the isothermal sound speed, $m_2 = 1/\sqrt{7}$, and at the adiabatic sound speed $m_2 = 1$. The narrow lines and dark gray area are the same as those in Newman & Axford (although note that they use isothermal, rather than adiabatic, Mach numbers). The bold lines and lighter shaded area are also allowed. In particular, note the short section of the $m_1 > 1$ curve with between the horizontal dotted lines: this section is the locus of transonic RF.

tions is at the adiabatic sound speed, whereas in a strictly isothermal flow it is at the isothermal sound speed. We find that, where thermal timescales are short in an accelerating flow, a ‘wide’ range of solutions near the adiabatic sound speed derive from a ‘few’ at the isothermal sound speed: it is apparent that in the limit, these ‘few’ solutions can become the singular isothermal transonic solution.

In the theory of multifluid MHD shocks, smooth transonic solutions are also found for strong cooling (Chernoff 1987; Flower & Pineau des Forêts 1987; Roberge & Draine 1990). In these shocks, the solution adapts to pass through a downstream (saddle type) sonic point using the freedom of manoeuvre allowed by an upstream viscous subshock (J-type) or nodal sonic point (C^* -type), rather than as discussed here.

There has been little discussion of RF since the work of NA, since in the winds of main sequence stars they will occur, if at all, at large radii, and thus at densities and temperatures so low that they will be broadened beyond recognition by advection. The interstellar medium in the vicinity of strongly ionizing stars does not generally reach an equilibrium state in the stellar lifetime – an IF is still being driven out into the surrounding medium when the star dies. However, in recent work we have discussed how a near-equilibrium state may be found in the youngest of these stars, observed as ultra compact H II regions (Dyson 1994; Williams & Dyson 1994; Dyson, Williams & Redman 1995).

Mass loading in the near vicinity of the young stars traps the IF at a scale of 0.1 pc, turning it into a RF through which gas passes at high density. In some objects, the mass-loaded stellar wind may remain supersonic at all radii – however, if the mass loading is strong enough the flow will shock. Detailed hydrodynamical simulations (Williams, Redman & Dyson, in preparation) confirm that transonic RF are frequently a component of the equilibrium flow. Such regions may be a significant source for partially ionized gas in the interstellar medium.

We note briefly that the discussion here also applies to the structure of H II region IF as they undergo the transition from R-type to D-type (Mason 1980). A shock first forms, as a (quasi-) steady part of the IF structure, at the minimum of the adiabatic Mach number in the R-type front when this reaches unity; initially, the post-shock flow is in the unstable range. In this region, however, the heating and cooling in the transonic flow are rather weak. More significantly, as the resultant strong D-type front weakens, the velocity relative to the front downstream in the H II region will eventually reach the unstable range. In this case, there is a significant chance that solutions will be missed in steady-state integrations.

ACKNOWLEDGEMENTS

We thank Robert Cannon, Sam Falle, Franz Kahn and Matt Redman for helpful discussions. The referee's thoughtful report improved the exposition and made us aware of analogous results in the literature on MHD shocks. This work was supported by PPARC through the Rolling Grant to the Astronomy Group at Manchester (RJRW).

REFERENCES

- Axford W.I., 1961, *Phil. Trans. R. Soc. London, A*, 253, 301
 Beltrametti M., Tenorio-Tagle G., Yorke H.W., 1982, *A&A*, 112, 1
 Chernoff D.F., 1987, *ApJ*, 312, 143
 Churchwell E., 1990, *A&AR*, 2, 79
 Cohen S.D., Hindmarsh A.C., 1994, *CVODE User Guide*, netlib archive
 Dyson J.E., Williams D.A., 1980, *The Physics of the Interstellar Medium*, Manchester University Press, Manchester
 Dyson J.E., 1994, in Ray T.P., Beckwith S.V., ed, *Lecture Notes in Physics 431: Star Formation Techniques in Infrared and mm-wave Astronomy*, Springer-Verlag, Berlin, p. 93
 Dyson J.E., Williams R.J.R., Redman M.P., 1995, *MNRAS* in press
 Fall S.M., Rees M.J., 1985, *ApJ* 298, 18
 Field G.B., 1965, *ApJ*, 142, 531
 Flower D.R., Pineau des Forêts G., 1987, *MNRAS*, 224, 403
 Frank A., Noriega-Crespo A., Balick B., 1992, *AJ* 104, 841
 Goldsworthy F.A., 1961, *Phil. Trans. R. Soc. London, A*, 253, 277
 Kahn F.D., 1954, *Bull. Astr. Inst. Netherlands*, 12, 187
 Mason D.J., 1977, Ph.D. Thesis, University of Manchester
 Mason D.J., 1980, *A&A*, 92, 117
 Mallik D.C.V., 1975, *ApJ*, 197, 355
 Newman R.C., Axford W.I., 1968, *ApJ*, 151, 114
 Osterbrock D.E., 1989, *Astrophysics of Gaseous Nebulae and Active Galactic Nuclei*, University Science Books, Mill Valley, CA
 Parker E.N., 1958, *ApJ*, 128, 664
 Roberge W.G., Draine B.T., 1990, *ApJ*, 350, 700

Williams R.J.R., Dyson J.E., 1994, *MNRAS*, 270, L52

This paper has been produced using the Royal Astronomical Society/Blackwell Science L^AT_EX style file.